S & M 4241

# Optimized Thermal Error Prediction and Real-time Compensation in Computer Numerical Control Milling Machines Using Neural Networks and Advanced Sensor Selection

Dang-Khoa Nguyen, 1,2 Hua-Chih Huang, 1\* and Zhong-Ming Hsu1

<sup>1</sup>Department of Mechanical Engineering, National Kaohsiung University of Science and Technology,
Kaohsiung 807618, Taiwan

<sup>2</sup>Faculty of Engineering and Technology, Nong Lam University,
Ho Chi Minh City 700000, Vietnam

(Received August 25, 2025; accepted November 20, 2025)

*Keywords:* thermal error (TE), thermal compensation (TC), back propagation neural network (BPNN), K-means, PCA+K-means

In this study, we developed a thermal error prediction (TEP) model and employed the error compensation in real time in a computer numerical control (CNC) milling machine with three axes in actual cutting operations. Thirty-three PT-100 sensors were used in each critical part of the machine to collect temperature data during cutting. K-means was adopted to select eight crucial temperature sensors from the 33 temperature sensors, and PCA+K-means was used to determine seven critical temperature sensors from the 33 sensors to apply a model for TEP. In this study, we made the prediction model from a back propagation neural network (BPNN). The number of sensors chosen as the critical temperature sensors constitutes the input layer of the BPNN. In contrast, the three neurons in the output layer represent the deformation of X, Y, and Z. After training the model to predict errors, it is brought into the control system for real-time TEP. We conducted a 6 h actual cutting experiment to verify the effect of error compensation, and the average three-axis thermal error was decreased from 50 to 14 µm by the K-means selection method. The PCA+K-means selection method reduced the average thermal three-axis error from 50 to 11 μm as compared with the previous measurements. The results show that these two methods can effectively improve the machining accuracy of the workpiece by combining the BPNN model with a compensated real-time TEP model.

#### 1. Introduction

In the era of the prevalence of the processing manufacturing industry, with the increasing degree of automation and the development of tooling machines to move in a high-speed, high-precision direction, processing accuracy has become the most significant problem to explore. Numerous factors affect the accuracy of the machining process. The errors of computer numerical control (CNC) machine tools when machining can be categorized into the following

five types: (1) geometrical errors created by the assembly and manufacturing process; (2) thermal distortion errors related to internal and external heating sources; (3) the deformation error caused by reaction force that resulted from material cutting; (4) the control error caused by the control system, i.e., positioning error, and digital control error compensation algorithm; and (5) the machine tool vibration at high frequencies and tool wear. Thermal deformation (TD) has contributed the highest level of manufacturing error and accounted for more than 70% of it.<sup>(1)</sup> The machine part will undergo TD during reworking, changing the workpiece's and tooltip's relative location, leading to TE.

In compensation for TE, modeling technology is emphasized. The experimental modeling method, which uses statistical theory to examine temperature and TE, is the most widely used technique for modeling TE. Multiple temperature sensors are typically positioned on the machine tool to collect data for error modeling. However, it is necessary to filter the temperature variables throughout the modeling process. The presence of numerous temperature variables will significantly impair the modeling accuracy as a result of collinearity. However, the compensation process will be ineffective if important regions are not selected as variables for the model. Lo et al. (2) used coordinates to measure error components and proposed a temperature sensor optimization method that eliminated the co-linearity problem through correlation grouping. Three search cycles provided a fast path to obtain the best decision, and the most significant residual TE was reduced from 20 to 2.2 µm by selecting 4 out of 46 sensors. Zhang et al. (3) used a fuzzy similarity matrix to filter temperature sensors and experimented with a precision horizontal milling machining center. This experiment selects seven temperature variables as input from 29 temperature sensors monitoring the device model. Then, a multivariate regression analysis model was applied to build a model for thermal compensation, and the model accuracy can reach the range of  $-1.3-1.6 \mu m$ . Ming et al. (4) conducted thermal error prediction (TEP) experiments utilizing a CNC vertical milling center Leaderway V-450 and classified temperature variables using a fuzzy clustering method to acquire important and logical categories, after which crucial temperature measurement points were obtained for each kind on the basis of the gray correlation between TE and temperature variables. Next, nonsignificant temperature data were removed, and various co-linearity issues were resolved using a stepwise regression technique. Ten temperature sensors were lowered to two, and the ideal temperature sensitivity points were used to build the TEP model. Lou et al. (5) utilized a fuzzy clustering method to screen out the sensitivity of temperature issues, and seven temperature points were chosen from 27. A BP neural network model was applied to build a model for TEP. The average error before the TE compensation was 4.5868 µm, and after the TE compensation, the average error was reduced to 1.5633 µm, which was 65.92% lower. Ramesh et al. (6) used an artificial neural network (ANN) and support vector machine (SVM) to perform a comparison from the TEP model. They showed that the training time and prediction accuracy of the SVM model were better than those of the ANN model, and the thermal inaccuracy dropped from -20 to -60 μm to 2 to 4 μm. Horejš *et al.*<sup>(7)</sup> compensated for real-time TE using a horizontal milling center as a tester, used heat transfer functions (TTFs), and performed a comparison with multiple linear regression (MLR), where the machine's temperature and spindle speed serve as the adjustment algorithm's inputs. The prediction model is tested at spindle speed and machine temperature,

and the findings demonstrate that the TTF model minimizes the TE by more than 75% as compared with the MLR model. Wang *et al.*<sup>(8)</sup> deployed particle swarm optimization (PSO) to improve the back propagation neural network (BPNN). The hidden layer node and layer counts of the BPNN were optimized by including the PSO method to train the local network effectively. The PSO algorithm is applied to maximize the number of hidden layer nodes and layers of the BPNN and network out of the local optimal trap and improve flexibility. PSO also improves the weight and threshold of the BPNN. According to the results, the PSO-BPNN can reduce the TEP error on the main axis in the *z*-direction from 6.74 to 1.82% in the training range.

In this study, first, we used temperature sensors at critical points where the temperature changes considerably in various parts of the machine to collect the temperature data generated during the operation of the device:

- (1) Method 1: K-means clustering (K-means) filters the best combination of temperature sensing points.
- (2) Method 2: Principal component analysis (PCA) and K-means are used to select critical temperature sensors, which can accurately reflect the variation pattern between TE and the temperature of the machine, and improve the prediction accuracy of the TE model.
- (3) The BP modeling approach was later used to construct the error prediction model. After completing the prediction model, the machine controller reads from the model for real-time error compensation using the controller compensation method to calculate the error prediction model.

## 2. TD Principle of Three-axis CNC Milling Machine

## 2.1 Structure of three-axis CNC milling machine

The load for this research is the TMV-720A three-axis CNC milling machine manufactured by Tung Tai Precision Machinery Co., which mainly comprises a spindle box, table, slide, column, base, and so forth. The TMV-720A three-axis CNC milling machine has travel strokes of 720, 480, and 530 mm for the X-, Y-, and Z-axes, respectively, a rapid feed of 48 m/min for the three axes, a table size of 800  $\times$  480 mm, a maximum table load of 500 kg, and a maximum spindle speed of 8000 rpm.

The controller used in the three-axis CNC milling machine is the 21 MB controller from Suntech. The 21 MB controller is equipped with the Yaskawa bus communication control method, which solves the timing problem of the traditional pulse-type general-purpose controller in multi-axis motion control and provides reasonable simultaneous control and timeliness.

## 2.2 Heat source analysis of three-axis CNC milling machine

Milling machines generate many heat sources owing to the long operation time, and these heat sources are transmitted to different machine components in various ways, causing the temperature of the machine parts to rise and resulting in the TD of the parts. Common machine heat deformations can be divided into two types of heat elongation and heat lift, as shown in

Fig. 1, which shows the machine heat elongation and heat lift, thus causing the deterioration of machining accuracy.

Generally, the heat sources of a tool machine can be divided into two major groups: internal and external. The internal heat source comes from the heat generated during the operation and processing of the machine body. When the spindle rotates, the heat from the spindle is mainly generated by the spindle motor operation and the frictional heat of the bearings. The feeding system's primary heat source is the heat created by the motor operation, the frictional heat created by the movement of the ball and nut seat in the ball screw, the friction caused by the heat of the front bearing and rear, and the thermal friction of the linear slider. External heat sources affect the TD of the spindle and feed system heat sources. External heat sources mainly include the amount of heat generated by the peripheral devices on the CNC machine tool, the environment temperature change, and human error (the amount of heat generated by personnel and the temperature change caused by frequent access). These eventually cause the milling machine tool tip displacement because of the heat deformation, the so-called TE, as shown in Fig. 2, which illustrates the cause of the machine's temperature error.

#### 2.3 Establishment of temperature sensor system

The position of the temperature sensor installation considerably affects the TE compensation and prediction accuracy. Because of the spindle cantilever extension and bending deformation brought on by heat sources from the spindle motor, cantilever, column, and so forth, the CNC milling machine experiences the most significant TD. To monitor the TD temperature of the CNC milling machine, the best location to install temperature sensors is determined to be the main heat sources or areas of extreme temperature changes, such as the spindle box, drive motor, slider, and ambient-temperature of work floor.

In this study, we used 33 PT-100 temperature sensors to monitor the temperature changes on the CNC milling machine, as shown in Fig. 3. The ambient temperature was monitored by the 33rd sensor among them as the data needed to construct the model for predicting TE. The schematic of the implementation diagram of the real-time compensation of TD is depicted in Fig. 4.

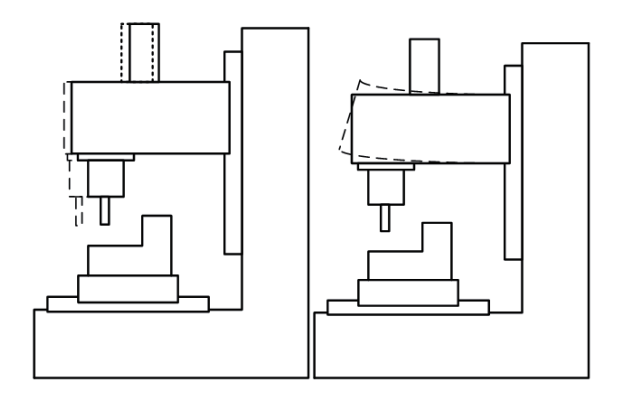


Fig. 1. TD occurs in milling machines.

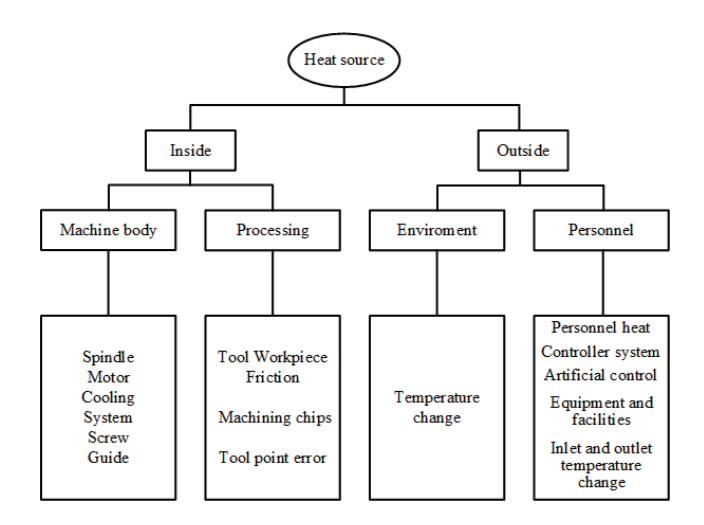


Fig. 2. TE in the machine.

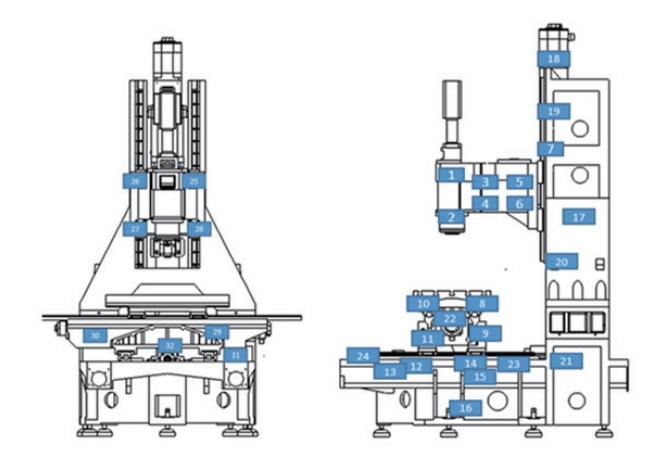


Fig. 3. (Color online) TE in the machine.

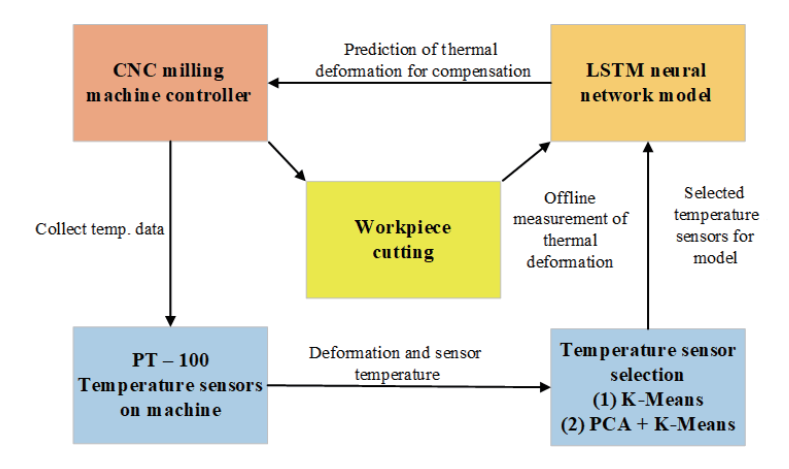


Fig. 4. (Color online) Implementation diagram of real-time compensation of TD.

## 3. Optimization of the Temperature Sensor Method

#### 3.1 K-means

The K-means of fuzzy cluster analysis is used for cluster selection because this method is simple, and only the representative sensors in each cluster are identified to represent the characteristics of the sensors in that cluster. Fuzzy cluster analysis is a system analysis based on the comparability between the sequences of system characteristic parameters, where similar variables are first grouped into the same class. Then, a representative variable from each class is selected as the independent variable. K-average clustering is an unsupervised machine learning algorithm that uses the target function to find the best cluster representatives. Then, the distance between the data and the cluster representatives is used to do the clustering; thus, the distance between the data and the cluster representatives is important. The line length of a segment between two locations in space is known as the Euclidean distance. The following is the computational step of K-means:<sup>(9)</sup>

- (1) Randomly set the number of k clusters to be divided.
- (2) Arbitrarily generate k clusters and determine the cluster centers.
- (3) Determine the Euclidean distance between each data point and the centers of the *k* clusters for each data point.
- (4) Each data point should be assigned to the cluster center nearest to it.
- (5) Compute the updated centroid of the cluster.
- (6) Repeat steps 3–5 until all the cluster centers no longer have much change (convergence).

The goal of K-means is to minimize the target function so that the error within the cluster is as small as possible, as shown in Eq. (1):

$$J(z,a) = \sum_{i=1}^{k} \sum_{x_j \in X_i} \|x_j - a_i\|^2 = \sum_{i=1}^{k} \sum_{j=1}^{n} z_{ij} \|x_j - a_i\|^2,$$
(1)

where J(z, a) is the target function, k is the size of the clusters,  $x_j$  is one of the data sets,  $a_i$  is the cluster centroid, and  $z_{ij}$  is the European Distance.

#### 3.2 Sum of squares error (SSE)

Owing to the unsupervised nature of K-means, the number of clusters that must be divided varies depending on the circumstances. As such, the question of how many clusters must be separated arises. In this study, SSE determines the number of bins. *SSE* will decrease considerably when the clusters are smaller in size than the actual cluster. When the size of the clusters approaches the real number of clusters, the decline will become flat, which is a turning point, so there is an "elbow point," which is the optimal number of clusters, (10) as shown in Eq. (2).

$$SSE = \sum_{i=1}^{k} \sum_{p \in C_i} |p - m_i|^2$$
 (2)

 $C_i$  is the *i*th group, p is the data point in  $C_i$ ,  $m_i$  is the group center of  $C_i$ , and SSE is the aggregation error, representing the good or bad aggregation.

## 3.3 PCA

There are many features available for data grouping. If too many features (dimensions) are input for grouping, the grouping effect will be poor and the operation speed will be slow. The PCA method can solve the processing of multidimensional (feature) data. After processing, most of the data information quantity can be retained. This method can retain the quantity of all the data characteristics and solve the problem that the feature selection may take a long time for trial and error.

There is a certain correlation between different data. Training more data, coupled with the correlation between data, will increase the complexity of the analysis problem. However, PCA is a way to restrict the dimension of data correlation as much as possible, seeking to combine the original huge data into a group of unrelated comprehensive data and reflect the original data information.

The calculation steps of PCA are as follows. (11,12)

(1) First, sort out a large amount of data and create a data matrix X:

$$X = \begin{bmatrix} x_{11} & \dots & x_{1p} \\ \vdots & \ddots & \vdots \\ x_{n1} & \dots & x_{np} \end{bmatrix}, \tag{3}$$

where p is the variable value of each sample and n is the total number of samples.

(2) The covariance of the variables i and j is

$$S_{ij} = \frac{1}{2} \sum_{k=1}^{n} \left( x_{ki} - \overline{x_i} \right) \left( x_{kj} - \overline{x_j} \right). \tag{4}$$

(3) The correlation coefficient represents the relationship between *i* and *j*:

$$r_{ij} = \frac{s_{ij}}{\sqrt{s_{ii}} \sqrt{s_{jj}}} = \frac{\sum_{k=1}^{n} (x_{ij} - \overline{x_i})(x_{kj} - \overline{x_j})}{\sqrt{\sum_{k=1}^{n} (x_{ki} - \overline{x_i})^2 \sum_{k=1}^{n} (x_{kj} - \overline{x_j})^2}}.$$
 (5)

(4) Equation (5) gives the sample correlation matrix. The correlation matrix is the covariance matrix following variable standardization:

$$R = \begin{bmatrix} 1 & r_{12} & \cdots & r_{1p} \\ r_{21} & 1 & \cdots & r_{2p} \\ \cdots & \cdots & \cdots \\ r_{p1} & r_{p2} & \cdots & 1 \end{bmatrix}.$$
 (6)

(5) Finally, the first p' principal components are selected through the eigenvalue  $\lambda$  of the covariance matrix R:

$$\sum_{i=1}^{p} \lambda_i / \sum_{i=1}^{p} \lambda_i \ge 0.80. \tag{7}$$

 $\sum_{i=1}^{n} \lambda_i$  is the sum of variances of all variables. When a new variable contributes more,  $\lambda$  will be larger.

To reduce the amount of work involved in the analysis, the principal components in the PCA are arranged according to variance. This allows for discarding some main components and identifying the original variables in only the first few principal components with larger variances. To ensure that the comprehensive evaluation results are unaffected by the workload-saving removal of important indicators, the 80% cumulative contribution rate concept is used when utilizing the PCA approach.

## 4. Screening of Critical Sensors in Temperature Sensors

## 4.1 Measurement experiments on TD

In this study, to obtain the thermal equilibrium and the deformation data when cutting, the experiment was run for 8 h, and the cutting operation was performed every 2 h to obtain the TD data of the three axes of the machine, which was planned by running and stopping the engine. In the processing part, we used the rotary cutting method for the trajectories of the *X*-, *Y*-, and *Z*-axes, as depicted in Fig. 5.

The cutting material is aluminum block AL6061, the workpiece is 100 mm in length, 100 mm in width, and 100 mm in height, and the tool used is the  $\phi$ 10 three-flute tungsten carbide end mill. To determine the X-, Y-, and Z-axes' deformation, the block was divided into five sides, and the first and third sides were applied to determine the deformation of the Y-axis; the deformation of the X-axis was measured using the second and fourth sides, and the deformation of the Z-axis was measured using the top side as shown in Fig. 6.

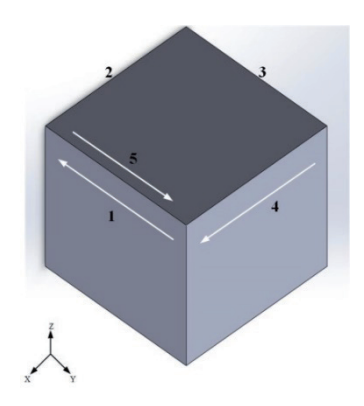


Fig. 5. Five-face cutting workpiece path diagram.

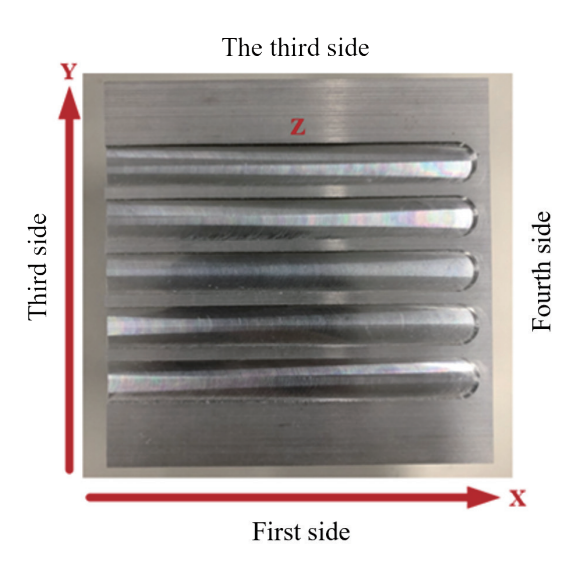


Fig. 6. (Color online) Aluminum block measurement setting.

After the experiment started, a set of TD cutting and measurement procedures was designed to obtain the temperature change and the TD data on the three axes while cutting the CNC milling machine with the three axes.

To obtain the thermal balance of the machine and the TD data of the time machine cutting, the experiment was run empty for 8 h, and the cutting operation was carried out every 2 h to obtain the TD data of the three axes of the machine, which was planned by running empty and stopping the machine. After the cutting process was completed, the final dimensional measurement of the cutting workpiece was carried out using a three-dimensional measuring instrument to obtain the error of the three axes X, Y, and Z at each speed. Figure 7 shows the experimental diagram of TD. The settings for the machining of this flow chart are as follows: the spindle speed ranges from 5000 to 7000 rpm, the feed rate is 3000 mm/min, and the X-, Y-, and Z-axes of travel are 0--720, 0--430, and 0--500 mm each, respectively.

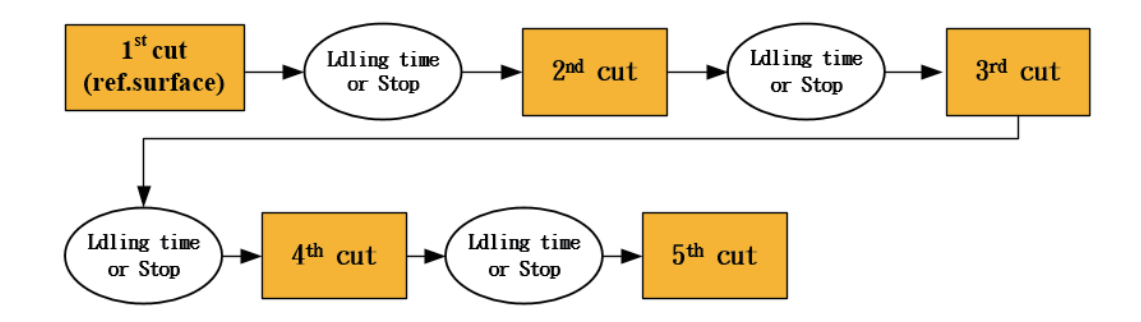


Fig. 7. (Color online) Experimental diagram of TD.

## 4.2 K-means-selected key temperature sensors

In this study, K-means was first used to screen key sensors, and *SSE* was used to find the number of clusters, as illustrated in Fig. 8. Then, the relationship between temperatures was used to group sensors, and the sensor with the greatest correlation coefficient between temperatures in each group was selected as the key sensor. Finally, seven temperature sensors and the ambient temperature were selected as sensors 2, 3, 17, 18, 23, 26, and 31. In addition, eight key temperature sensors plus the ambient temperature Ta were selected as the temperature data input to the neural network. Figure 9 shows the location diagram of key temperature sensors selected by K-means in the machine. Table 1 indicates the placements of eight key temperature sensors.

## 4.3 PCA+K-means-selected key temperature sensors

First, the temperature data were divided into 12 characteristic quantities: maximum, minimum, standard deviation, mean, 25th percentile, 50th percentile, 75th percentile, maximum minus minimum, temperature difference at 0–2, temperature difference at 2–4, temperature difference at 4–6, and temperature difference at 6–8. The results of the 12 characteristic quantities were analyzed by PCA, as shown in Table 2. From Table 3, the contribution rates are 0.026833 when there are three features and 0.00091 or less when there are four or more features, indicating that the amount of information on three features is sufficient, so it is decided to use three components to represent more than 99% of the data information.

After the PCA analysis of the three features, the K-means method was used to perform the grouping, first using *SSE* to determine the K-means into seven groups, as shown in Fig. 10. In seven groups, the sensor with the highest temperature correlation in each group was chosen as the key temperature sensor to represent the group. The selected temperature sensors are sensors 3, 6, 12, 18, 19, and 20, and the ambient-temperature sensor is Ta. The positions of these key temperature sensors correspond to the machine's location, as shown in Fig. 11. Table 3 shows the positions of the seven key temperature sensors.

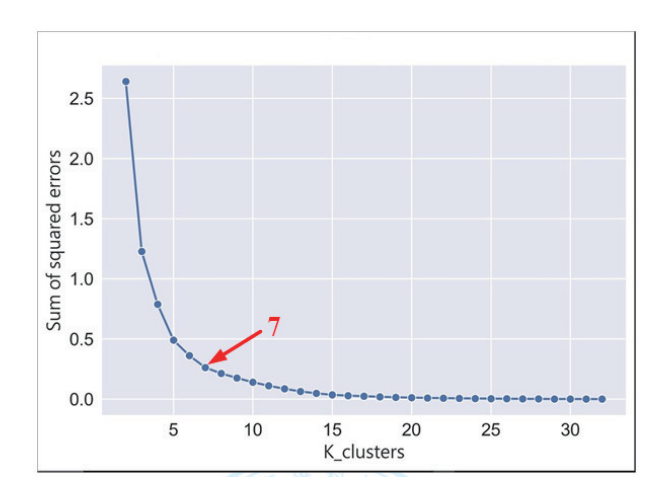


Fig. 8. (Color online) SSE is classified as Group 7.

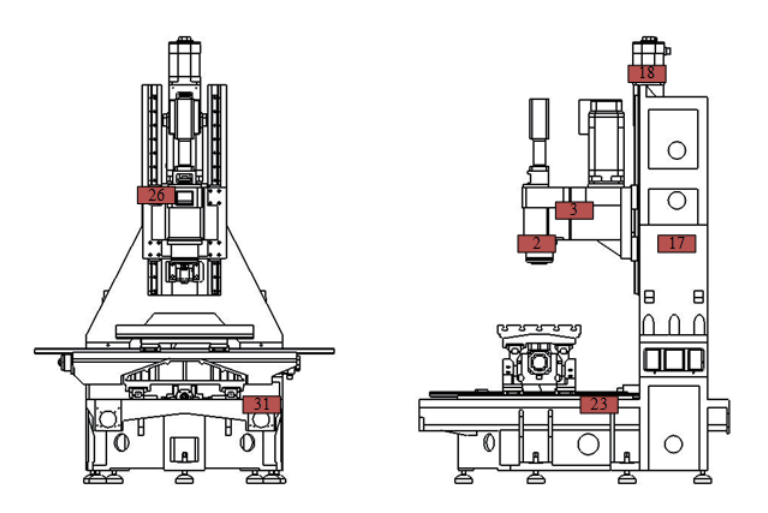


Fig. 9. (Color online) K-means selection of key temperature sensors in machine location 7.

Table 1 Locations of eight crucial temperature sensors.

	-8 I	
K-means-selected key temperature sensors		
Sensor	Location	
2	Spindle head	
3	On cantilever	
17	Column	
18	Z-axis motor base	
23	<i>Y</i> -axis bearing	
26	Z-axis slider	
31	<i>X</i> -axis motor base	
Ta	Ambient temperature	

Table 2
Temperature data were classified into 12 characteristic components of the PCA cumulative contribution rate (CR).

Cumulative CA of PCA principal component			
	CA	Cumulative CA	
1	0.870214	0.870214	
2	0.101288	0.971502	
3	0.026833	0.998335	
4	0.00091	0.999245	
5	0.000308	0.999553	
6	0.000282	0.999835	
7	6.97E-05	0.999905	
8	4.85E-05	0.999953	
9	2.86E-05	0.999982	
10	1.64E-05	0.999998	
11	1.8E-06	1	
12	1.05E-33	1	

Table 3 Locations of eight crucial temperature sensors.

DCA+IZ 1 + 11 +			
PCA+K-means-selected key temperature sensors			
Sensor	Location		
3	On cantilever		
6	Under cantilever		
12	Y-axis slider		
18	Z-axis motor base		
19	Z-axis bearing		
20	Z-axis bearing		
Ta	Ambient temperature		

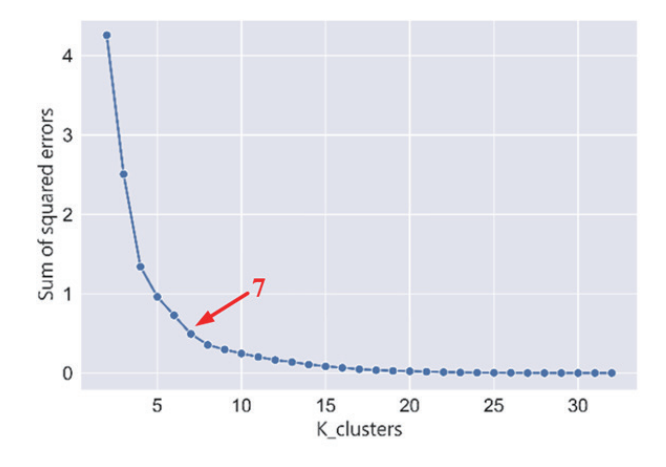


Fig. 10. (Color online) SSE is classified as Group 7.

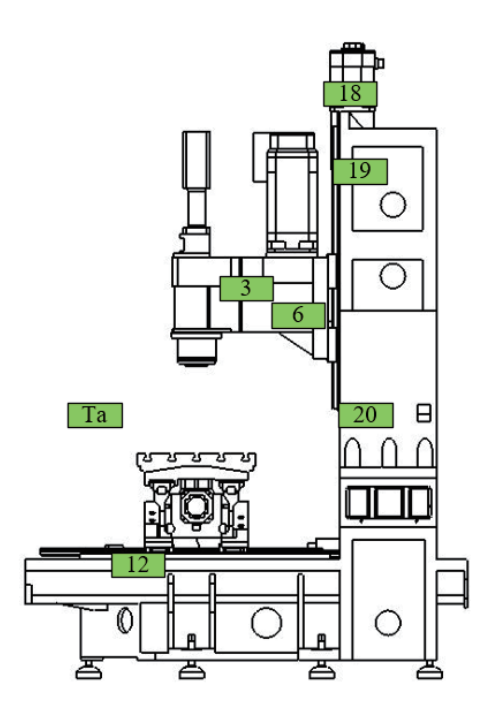


Fig. 11. (Color online) PCA+K-means selection of key temperature sensors in the machine location.

# 5. TEP Model Using Neural Network

#### 5.1 Architecture of BPNN

In this study, we built a TEP model from the BPNN. The BPNN uses BP as a learning algorithm, and its architecture is a multilayer perceptron. To supervise and train the prediction model, the BPNN, which is a feedforward multilayer neural network, uses the error back-propagation method to address the nonlinear problem between input and output. The relationship between TE and temperature at different points of the CNC milling machine is nonlinear, so the BPNN can solve this problem.

The algorithm of error inverse transmission is a combination of forward and reverse propagation processes, as shown in Fig. 12.<sup>(13,14)</sup>

- (1) The forward propagation process consists of weighting the data in the input layer by the hidden layer, processing the activation function, and then transmitting it to the output layer to calculate the output (real line).
- (2) On the other hand, when the output does not reach the target of the output layer, it will turn to reverse propagation and send the error back to the neurons of each layer along the original path, and improve it by modifying the weights so that the error can reach the tolerance error range and then stop (dashed line).

The backward propagation neural network realizes the adjustment process of forward and reverse transmission of data. The training steps of BPNN are as follows. (15–17)

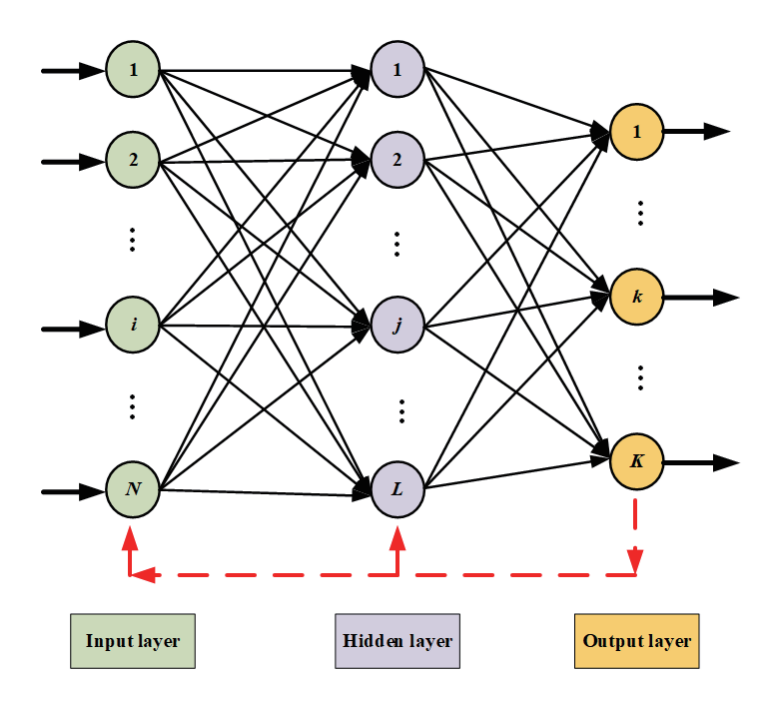


Fig. 12. (Color online) Schematic structure of BPNN.

- (1) Calculate the total number of neurons in each layer and the number of layers. Forward portion of the transmission to the input layer.
- (2) Randomly set the weights of the hidden and output layers.
- (3) Input the input and target output of the training data.
- (4) Calculate the outputs of the hidden and output layers.
- (5) Consider the calculation error function as  $E = \left(\frac{1}{2}\right) \sum (d_k y_k)^2$ . Part of BP:
- (6) Calculate the weight and offset corrections between layers (from back to front).
- (7) Update the weights of the output and hidden layers.
- (8) Repeat steps 3 to 7 until convergence (very low loss and almost no longer floating) or the end of the preset period (epoch).

# 5.2 TEP model building and training

Since the training of the TEP model requires big input and output data, the input data is the value of the key temperature sensor. In contrast, the output data is the three-axis TE obtained from the workpiece measurement. In this study, we used Python syntax as the experimental method for training the TEP model. Thermal data from the main temperature sensor and the corresponding three-axis TE are introduced into the model, and the BPNN is utilized to train the model for TEP. Big data were first divided into training and verification data. The temperature sensor and TD data from the three axes were divided into 70% training data and 30% verification data. The model for predicting error was obtained after training the training data model. Then, the verification data were inserted into the prediction model, and the prediction model error was

calculated. When the prediction error reached the expected target, the model was stored as the TEP model.

In this study, we used two methods to select key temperature sensors to construct and compare TEP prediction models. Method 1: K-means three-axis TEP findings are given in Fig. 13(a). The residual value of the three-axis TEP of K-means is shown in Fig. 13(b). Method 2: PCA+K-means three-axis TEP findings are given in Fig. 14(a). The residual value of PCA+K-means three-axis TEP is shown in Fig. 14(b). The data collation and comparison between Methods 1 and 2 are shown in Table 4.

From Table 4, the maximum prediction residual of the temperature sensor selected by the K-means method through BPNN simulation is  $4.7265 \mu m$ . The average of the three-axis residual

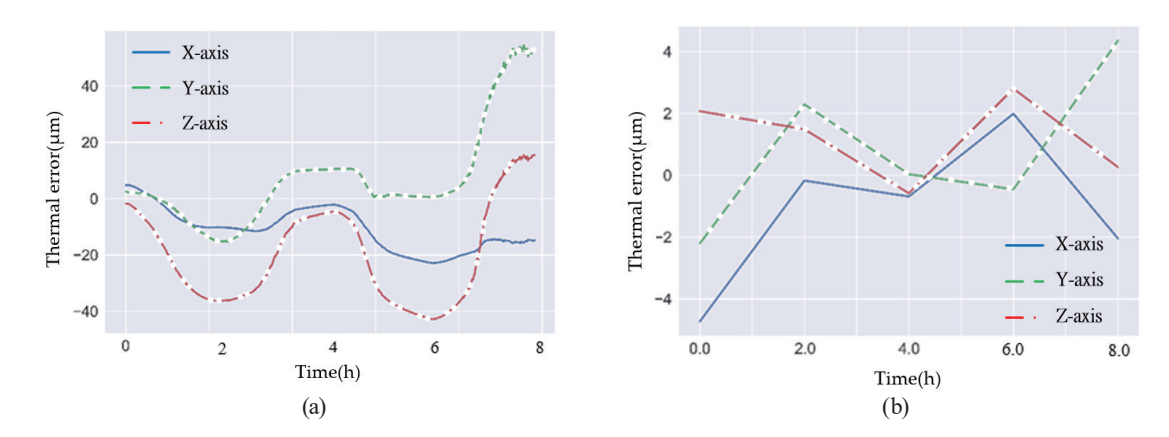


Fig. 13. (Color online) (a) Results of three-axis TEP by K-means and (b) residual value of the three-axis TEP of K-means.

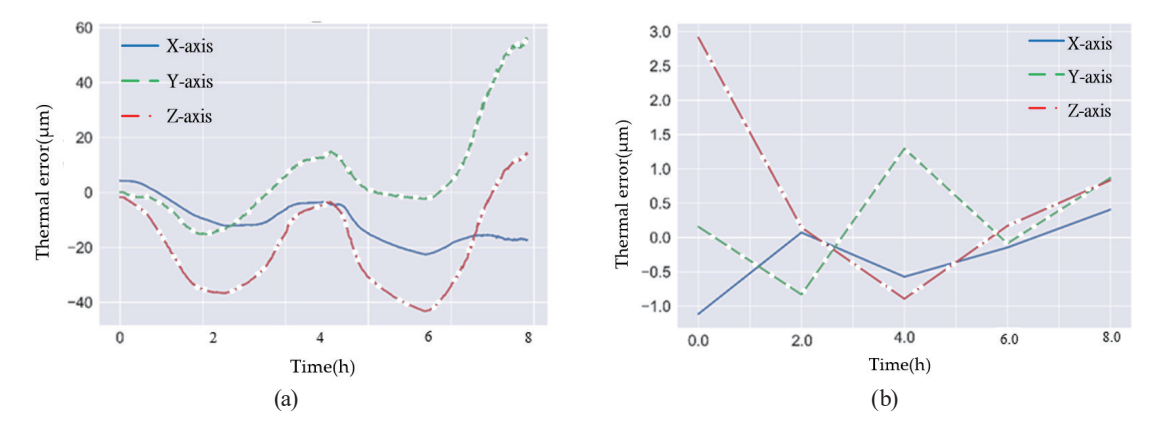


Fig. 14. (Color online) (a) Results of three-axis TEP by PCA+K-means and (b) PCA+K-means three-axis TEP residual value.

Table 4 Averages of three-axis triaxial TEP residuals for two methods.

Temperature sensor selection method	X-axis	Y-axis	Z-axis	Three-axis mean
remperature sensor selection method	(µm)	(µm)	(µm)	(µm)
K-means method	4.7265	4.3531	2.7982	3.9592
PCA+K-means method	1.1149	1.2941	2.9112	1.7734

is  $3.9592~\mu m$ , whereas the maximum prediction residual of the temperature sensor selected by the PCA+K-means method through BPNN simulation is  $2.9112~\mu m$ , and the average of the triaxial residual is  $1.7734~\mu m$ . It can be deduced that the model's prediction accuracy is improved by reducing the complexity and dimensionality of the data computation using PCA, and the prediction accuracy tends to improve.

## 6. TEP Model Real-time Compensation Experiment

When the TEP model calculates the estimation error, the controller must compensate for it in real time. In this study, the controller uses the OPC Unified Architecture (OPC UA), a machine-to-machine network transmission protocol applied in automation technology, to transfer the prediction model-estimated TEP of three axes to the controller for TE compensated for the three-axis CNC milling machine in real time. The configuration of a real-time compensation strategy for temperature errors is presented in Fig. 15, and real-time error compensation steps are depicted in Fig. 16.

In this study, we used the TE compensation prediction model completed by training to carry out the verification experiment of actual cutting processing. This experiment was carried out for 6 h, cutting once every 1.5 h and four times in total to obtain the amount of information after compensation. The spindle speed was set at 5000 rpm, the feed rate was 3000 mm/min, and the experimental conditions are presented in Fig. 17.

In Method 1, the temperature changes of the sensors screened by K-means are shown in Fig. 18, which illustrates the temperature variations of sensors 2, 3, 17, 18, 23, 26, 31, and Ta within 6 h in experiment. The compensation results of the X-, Y-, and Z-axes, using the model for predicting error, are depicted in Table 5. The TE compensation analysis shows that the average TE of the X-axis has decreased from 28 to 10  $\mu$ m, the average TE of the Y-axis has decreased from 79 to 16  $\mu$ m, and the average TE of the Z-axis has decreased from -42 to -15  $\mu$ m.

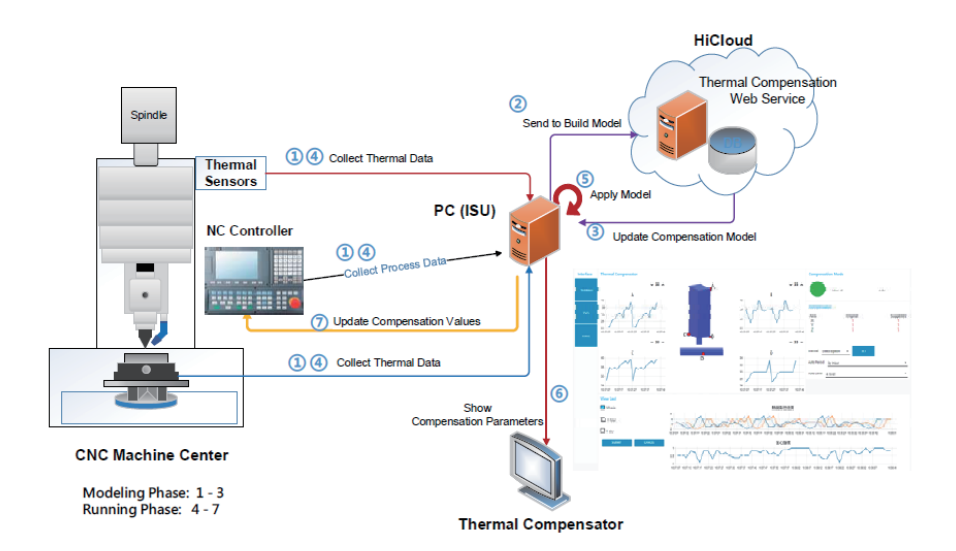


Fig. 15. (Color online) Configuration of a real-time compensation strategy for temperature errors.

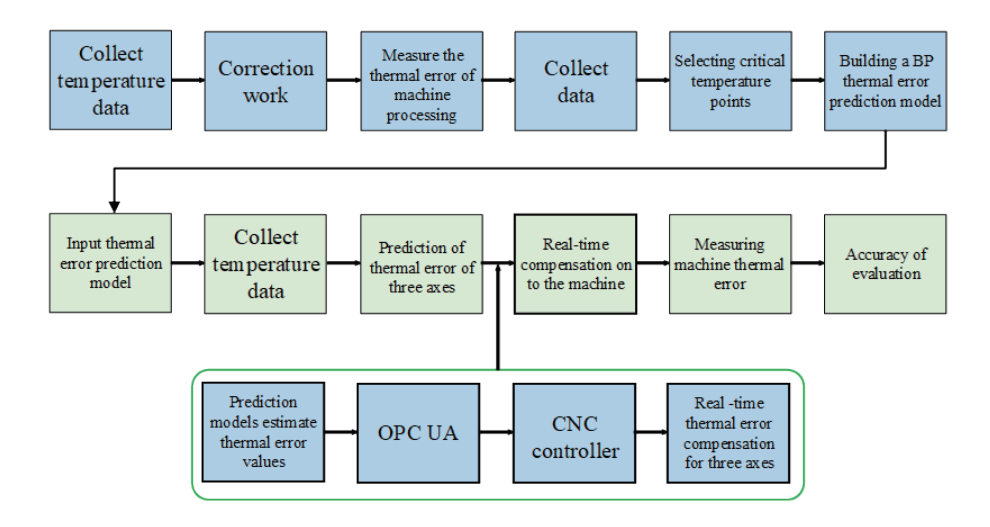


Fig. 16. (Color online) Real-time error compensation steps.

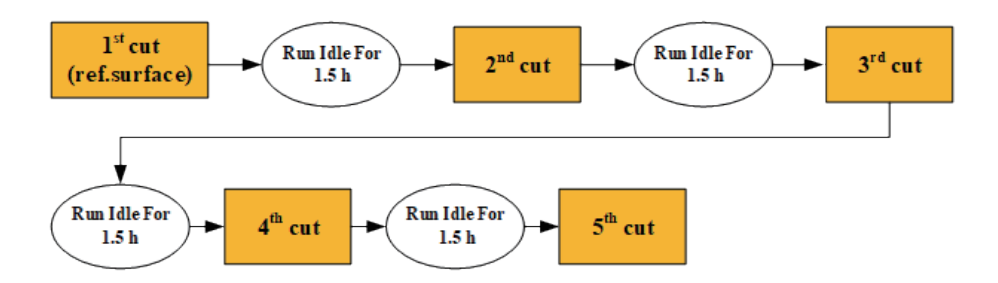


Fig. 17. (Color online) Working conditions of the actual cutting heat error compensation experiment of 6 h of run.

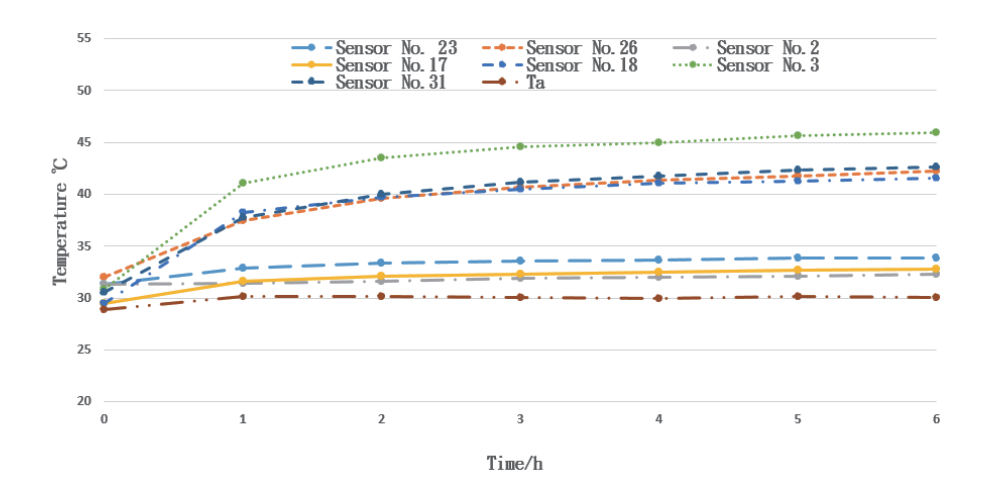


Fig. 18. (Color online) Method 1: Temperature changes of the key temperature sensors selected by K-means running empty for  $6\,h$ .

Table 5
Method 1: TE values of key temperature sensors screened by K-means before and after experimental compensation.

Axial direction	Dua a again a tima (h)	No real-time compensation	Real-time compensation
Axial direction	Processing time (h)	for TE (µm)	for TE (µm)
	1.5	11.9	9.8
v ·	3	24.2	9.3
X-axis	4.5	35.9	10.8
	6	39.7	11.5
	1.5	52.5	4
Y-axis	3	82.2	12.5
I-axis	4.5	89.1	22.1
	6	90.3	26
Z-axis	1.5	-35.5	-3.4
	3	-38.3	-12.6
	4.5	-45.3	-18.3
	6	-49.7	-25.7

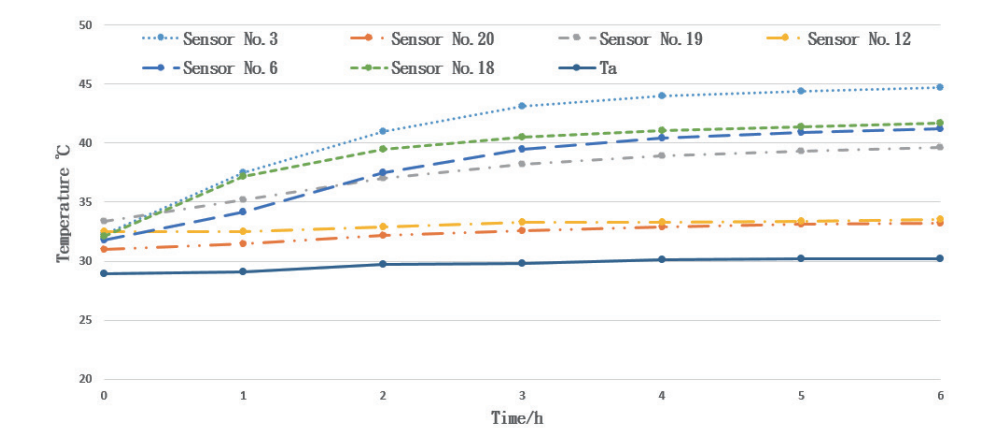


Fig. 19. (Color online) Method 2: Temperature changes of key temperature sensors screened by PCA+K-means after running empty for 6 h.

Table 6 Method 2: PCA+K means screening key temperature sensor TE values before and after experimental compensation.

Axial direction	Processing time (h)	No real-time compensation	Real-time compensation
Axiai direction		for TE (µm)	for TE (µm)
X-axis	1.5	11.9	5.3
	3	24.2	10.1
	4.5	35.9	15.2
	6	39.7	20.2
Y-axis	1.5	52.5	1.7
	3	82.2	7.3
	4.5	89.1	9.8
	6	90.3	13.9
Z-axis	1.5	-35.5	-1.3
	3	-38.3	-8.9
	4.5	-45.3	-17.7
	6	-49.7	-25

The temperature changes of the seven key temperature sensors screened by PCA+K-means, i.e., sensors 3, 6, 12, 18, 19, 20, and Ta running in air for 6 h, are presented in Fig. 19. Table 6 shows the *X*-, *Y*-, and *Z*-axis compensation results obtained using the model for predicting TE. The TE measurements before and after compensation indicate a significant reduction in average TE for each axis. Specifically, the average TE for the *X*-axis decreases from 28 (uncompensated) to 13 μm (compensated), the average TE for the *Y*-axis decreases from 79 (uncompensated) to 8 μm (compensated), and the average TE for the *Z*-axis decreases from -42 (uncompensated) to -13 μm (compensated).

Tables 5 and 6 show that the key temperature sensors screened by the two methods combined with the BPNN can effectively reduce TE. The three-axis average error of the key temperature sensor screened by K-means is 14 μm, and that of the key temperature sensor screened by PCA+K-means is 11 μm. The experiment proves that if PCA is carried out on big data first, the correlation between data can be avoided, thus causing complexity in training and analysis. Later, K-means is used to select key temperature sensors in groups as the BPNN input. The model for compensating TE can be more effective in the operation of the machine such that the machining accuracy of the device can be improved.

## 7. Main Findings and Conclusion

In this study, the K-means and PCA+K-means methods were employed to identify critical temperature sensors. A Python-based model was developed to predict TE, and the predicted three-axis TD was integrated into the machine controller via OPC UA for real-time compensation during machining. The main findings and conclusion are summarized as follows:

#### • Main Findings:

## A. Thermal Error Modeling:

- We developed a TEP model using BPNN to address the significant TD affecting CNC milling machines' machining accuracy.
- Optimized sensor selection by K-means and PCA effectively reduced the number of critical temperature sensors from 33 to 7, improving model efficiency and predictive accuracy.

## B. Accuracy Improvement:

- The PCA+K-means approach demonstrated superior performance, reducing the average residual error in the three-axis TEP model to 1.77 μm, compared with 3.96 μm with K-means alone.
- Real-time compensation experiments showed that PCA+K-means reduced thermal errors along the X-, Y-, and Z-axes to 13, 8, and -13 μm, respectively. This outperformed K-means, which achieved 10, 16, and -15 μm for the same axes.

## C. Experimental Validation:

• A 6 h cutting experiment validated the model's practical effectiveness. The PCA+K-means method achieved an average three-axis error reduction from 50  $\mu$ m (baseline) to 11  $\mu$ m, further confirming the efficiency of dimensionality reduction and clustering methods

## 8. Conclusion

This research highlights the critical role of integrating advanced sensor optimization methods and neural networks for real-time thermal error compensation in CNC milling machines. By employing PCA to reduce data dimensionality and K-means to optimize sensor placement, the proposed method significantly improved the accuracy of TEP and compensation. The findings underscore the importance of combining statistical and machine learning techniques to address manufacturing challenges, offering a robust solution for enhancing machining precision in real-world industrial applications.

#### References

- 1 J. Bryan: Ann. CIRP. **39** (1990) 645. <a href="https://doi.org/10.1016/S0007-8506(07)63001-7">https://doi.org/10.1016/S0007-8506(07)63001-7</a>
- 2 C. H. Lo, J. Yuan, and J. Ni: Int. J. Mach. Tools Manuf. 35 (1995) 1669. <a href="https://doi.org/10.1016/0890-6955(95)97296-C">https://doi.org/10.1016/0890-6955(95)97296-C</a>
- 3 T. Zhang, W. Ye, R. Liang, P. Lou, and X. Yang: Chin. J. Mech. Eng. 26 (2013) 158. <a href="https://doi.org/10.3901/CJME.2013.01.158">https://doi.org/10.3901/CJME.2013.01.158</a>
- 4 M. E. Ming, G. Y. Yun, D. L. Chun, and M. J. Chao: Int. J. Adv. Manuf. Technol. 74 (2014) 681. <a href="https://doi.org/10.1007/s00170-014-6009-y">https://doi.org/10.1007/s00170-014-6009-y</a>
- 5 P. Lou, N. Liu, Y. Chen, Q. Liu, and Z. Zhou: Int. J. Manuf. Res. 12 (2017) 338. <a href="https://doi.org/10.1504/1JMR.2017.086177">https://doi.org/10.1504/1JMR.2017.086177</a>
- R. Ramesh, M. A. Mannan, and A. N. Poo: Int. J. Adv. Manuf. Technol. 20 (2002) 114. <a href="https://doi.org/10.1007/s001700200132">https://doi.org/10.1007/s001700200132</a>
- 7 O. Horejš, M. Mareš, and L. Novotný: Procedia CIRP. 4 (2012) 67. https://doi.org/10.1016/j.procir.2012.10.013
- 8 J. Wang, T. Jiang, J. Shen, J. Dai, Z. Pan, and X. Deng: Instrumentation Mesure Métrologie. 19 (2020) 301. https://doi.org/10.18280/i2m.190408
- 9 F. Gao, C. Hei, J. Liu, Y. Li, and L. Shui: Int. J. Adv. Manuf. Technol. 114 (2021) 1385. <a href="https://doi.org/10.1007/s00170-021-06945-3">https://doi.org/10.1007/s00170-021-06945-3</a>
- J. Zhang, L. Liu, Y. Fan, L. Zhuang, T. Zhou, and Z. Piao: IEEE Access 8 (2020) 47797. <a href="https://doi.org/10.1109/access.2020.2979220">https://doi.org/10.1109/access.2020.2979220</a>
- 11 R. Christensen: Analysis of variance, design, and regression: applied statistical methods (CRC Press, 1996).
- 12 S. Katipamula, T. A. Reddy, and D. E. Claridge: J. Sol. Energy Eng. **120** (1998) 177. <a href="https://doi.org/10.1115/1.2888067">https://doi.org/10.1115/1.2888067</a>
- 13 P. Mukhopadhyay: Multivariate statistical analysis (World Scientific, 2009).
- 14 F. Z. Zhang, L. Q. Zhang, and H. L. Huang: Theory and Practice (Neural networks, Taiwan Donghua Co., Ltd, First Ed., 2003).
- 15 X. Wan, M. Lin, and H. Chen: Application and Practice of Fuzzy Theory (Rulin Book Company, First ed., 2008).
- 16 M. Straka, M. Mares, and O. Hoerjs: MM Sci. J. (2021). https://doi.org/10.17973/MMSJ.2021 11 2021173
- 17 D.-K. Nguyen, H.-C. Huang, and T.-C. Feng: Machines 11 (2023) 248. <a href="https://doi.org/10.3390/machines11020248">https://doi.org/10.3390/machines11020248</a>